

Original Research

N-acetyltransferase 10 Promotes Cervical Cancer Progression Via N4-acetylation of *SLC7A5* mRNA

Peili Liang^{1,2,†}, Dongmei Zhou^{2,†}, Jinrong Liao¹, Wujiang Lai^{1,3}, Xiujie Sheng^{2,*}, Yifeng Wang^{1,*}

Submitted: 27 September 2024 Revised: 18 December 2024 Accepted: 25 December 2024 Published: 20 February 2025

Abstract

Introduction: N-acetyltransferase 10 (NAT10) mediates N4-acetylcytidine (*ac4C*) mRNA modification and promotes malignant tumor progression. However, there has been limited research on its role in cervical cancer. This study aimed to decipher the role of NAT10 in cervical cancer. **Methods**: The prognostic value of NAT10 was explored using the cancer genome atlas (TCGA) database and immunohistochemistry of cervical cancer tissue. The biological actions of NAT10 in cervical cancer were investigated by cell proliferation, transwell, wound healing, and chicken chorioallantoic membrane assays. The therapeutic action of remodelin (a NAT10 inhibitor) was verified in a nude mouse model. Mechanistic analyses were conducted by RNA sequencing, ac4C dot blotting, acetylated RNA immunoprecipitation, quantitative PCR, and RNA stability experiments. **Results**: NAT10 was overexpressed in cervical carcinoma and its overexpression was associated with poor prognosis. NAT10 knockout impaired proliferative and metastatic potentials of cervical cancer cells, while its overexpression had the opposite effects. Remodelin impaired cervical cancer proliferation *in vivo* and *in vitro*. NAT10 acetylated solute carrier family 7 member 5 (*SLC7A5*) enhanced mRNA stability to regulate SLC7A5 expression. **Conclusions**: NAT10 exerts a critical role in cervical cancer progression via acetylating *SLC7A5* mRNA and could represent a key prognostic and therapeutic target in cervical cancer.

Keywords: NAT10; cervical cancer; progression; N4-acetylcytidine (ac4C); solute carrier family 7 member 5 (SLC7A5)

1. Introduction

Cervical cancer, one of the major threats to women's health globally [1,2], has consistently high incidence and mortality rates [3], especially in low- and middle-income countries [4,5]. Early-stage cervical cancer can be managed with radical surgery and adjuvant chemoradiotherapy. For recurrent and metastatic cervical cancer, effective treatment is lacking, leading to a 5-year survival rate of $\sim 17\%$ [6]. The addition of bevacizumab to conventional cisplatin plus paclitaxel chemotherapy can improve patients prognosis for cervical cancer, extending their life span by 3.7 months [7]. In addition, various immunotherapies have been developed to treat cervical cancer, which achieve a disease control rate reaching 52% [8,9]. Despite these advances, the effective treatment of recurrent and metastatic cervical cancer remains a formidable challenge. Therefore, it is key for exploring mechanisms underlying the development and occurrence of cervical cancer, and identifying effective drugs to attenuate cervical cancer progression.

Acetylation of N4-acetylcytidine (ac4C) [10], an epigenetic modification [11], has become a research hotspot in recent years. N-acetyltransferase 10 (NAT10) is primary enzyme that catalyzes ac4C modification on RNA molecules, thereby enhancing RNA stability and promoting its translation and expression [12–15]. An increasing number of literatures have reported that NAT10 is crucial in cancer development. For example, NAT10-mediated mRNA ac4C modification potentiates bladder cancer progression [13]. NAT10 facilitates cancer development via cell cycle modulation in non-small cell lung cancer [16]. NAT10 potentiates proliferative, migratory, invasive, and metastatic capacities of colorectal cancer cells by N4-acetylation and stabilizing ferroptosis inhibitor 1 mRNA [17]. NAT10 enhances cell proliferative ability by acetylating centrosomal protein 170 mRNA to increase translation efficiency in multiple myeloma [12]. Although mechanism of NAT10mediated ac4C modification of RNA has been extensively explored, mechanisms by which NAT10 modulates cancer, especially cervical cancer, is not well understood. Remodelin is a NAT10 inhibitor that was first reported by Larrieu

¹Obstetrics and Gynecology Center, Zhujiang Hospital, Southern Medical University, 510260 Guangzhou, Guangdong, China

²Department of Obstetrics and Gynecology, Guangdong Provincial Key Laboratory of Major Obstetric Diseases, Guangdong Provincial Clinical Research Center for Obstetrics and Gynecology; Guangdong-Hong Kong-Macao Greater Bay Area Higher Education Joint Laboratory of Maternal-Fetal Medicine; The Third Affiliated Hospital, Guangzhou Medical University, 510150 Guangzhou, Guangdong, China

³Department of Obstetrics and Gynecology, Shunde Hospital, The First People's Hospital of Shunde, Southern Medical University, 528300 Foshan, Guangdong, China

^{*}Correspondence: 2008691150@gzhmu.edu.cn (Xiujie Sheng); wangyifeng@smu.edu.cn (Yifeng Wang)

[†]These authors contributed equally. Academic Editor: Ilaria Baglivo

et al. in 2014 [18]. Remodelin can inhibit various tumors progression such as bladder cancer, and multiple myeloma [13,19,20]. Remodelin can also reverse adriamycin resistance in breast cancer [21,22]; thus, it may be a promising anticancer agent. However, remodelin's role in cervical cancer is poorly understood.

Solute carrier family 7 member 5 (SLC7A5) amino acid transporter is key for maintaining intracellular amino acid pool [23], which facilitates the uptake of nutrients by cancer cells. Recent evidence has implicated that SLC7A5 is overexpressed in several malignancies, such as colon and breast cancers, and its overexpression predicts poor prognosis [24–27]. As an oncogene, SLC7A5 is key for cancer cell progression [26]. SLC7A5 is associated with inflammatory tumor immune microenvironment and can predict response of patients with bladder cancer to immunotherapy, radiotherapy, and chemotherapy. Targeting SLC7A5 along with immunotherapy may be a potentially suitable therapeutic strategy [28]. Loss of SLC7A5 in kirsten rat sarcoma virus (KRAS)-mutant colorectal cancer alters intracellular amino acid homeostasis and reduces protein synthesis and mammalian target of rapamycin complex 1 (mTORC1)-S6K signaling. Although KRAS-mutant cells are resistant to rapamycin, silencing SLC7A5 sensitizes cells to mTORC1 inhibitors [25]. SLC7A5 potentiates proliferative ability by activating the AKT/mTORC1 signaling in breast cancer [29]. Modulating glutamine metabolic reprogramming of SLC7A5 potentiates anti-programmed cell death protein 1 efficacy in triple-negative breast cancer [30]. However, SLC7A5's role in cervical cancer is still unknown. Moreover, relationship between NAT10 and SLC7A5 in cancer has not been assessed.

To decipher underlying mechanisms of NAT10 in cervical cancer, we conducted a series of studies. Our research investigated the carcinogenic effects of NAT10 on cervical cancer by editing its expression. We demonstrated that NAT10 is overexpressed in cervical cancer and NAT10 overexpression is associated with poor prognosis in patients with cervical cancer. NAT10 overexpression markedly stimulated the proliferative and metastatic potentials of cervical cancer cells. Additionally, as a NAT10 inhibitor, remodelin attenuated proliferative and metastatic potentials of these cells, indicating its potential as an effective drug for treating cervical cancer. Mechanistic studies have suggested that NAT10 can positively regulate the ac4C acetylation level of SLC7A5 mRNA, thereby enhancing SLC7A5 mRNA stability and promoting the metastasis of cervical cancer. Therefore, NAT10 plays a key role in cervical cancer progression via the ac4C-SLC7A5 axis and thus may serve as a biomarker of cervical cancer.

2. Materials and Methods

2.1 Data Source and Preprocessing

We retrieved public gene expression data and full clinical annotations of Cervical Squamous Cell Carcinoma and Endocervical Adenocarcinoma (CESC) from The Cancer Genome Atlas (TCGA) (https://portal.gdc.cancer.gov/). This study enrolled 297 patients with cervical cancer, including 245 with squamous cell carcinoma of the cervix, 48 with adenocarcinoma of the cervix, and 4 patients with other pathological types. The baseline data is shown in Supplementary Table 1. The transcripts per million (TPM) format was log2 transformed and processed for analysis using R version 4.2.2 (Lucent Technologies, Murray Hill, NJ, USA). Using the function "surv categorize" of R package "survminer" (v0.4.9), the expression levels of NAT10 and SLC7A5 mRNA were divided into "high" or "low" groups. Survival analysis was carried out for patients with CESC using the expression data of tumors with "survminer" and the R package "survival" (v3.4.0), with ordinate representing survival rate and abscissa representing survival time. The p values were adjusted for multiple testing using the Benjamini-Hochberg method.

2.2 Immunohistochemistry of NAT10

A cervical cancer tissue microarray (HUteS136Su01, Shanghai Outdo Biotech Co, China) was dewaxed in xylene for 20 minutes; then hydrated in different gradients of ethanol for 5 minutes each. Following this, it was subjected to high-pressure fixation with sodium citrate for 5 min followed by blocking with 5% bovine serum albumin (BSA, CCS30014.01, MRC, Cincinnati, OH, USA) for 1 hour. Slides were dried, and NAT10 monoclonal antibody (1:100, SC-271770, Santa Cruz, Dalas, TX, USA) was incubated at 4 °C overnight. Slides were incubated with the mouse secondary antibody (1:5000, SA00001-1, Proteintech, Chicago, IL, USA) at room temperature for 0.5 h. After incubation, DAB (DA1010, Beijing Solaibao Technology Co., LTD, Beijing, China) was added for 3-5 minutes to lightly counterstain with hematoxylin. Staining intensity was measured using H-score method as described previously [13]. In short, scoring was based on percentage and frequency of positive staining cells as follows: 0 indicates no positive staining cells; 1–100 indicates 1–100% of cells stained. Staining intensity was scored as follows: 0 represents no staining, 1 represents weak positive staining, 2 represents medium positive staining, and 3 representes strong positive staining.

2.3 Cell Culture and Reagents

SiHa and CaSki human cervical cancer cells were purchased from Procell Company (Wuhan, China). C33A and HeLa human cervical cancer cells were kindly donated by Professor Zhang Bingzhong. The cell lines were cultured in Dulbecco's Modified Eagle Medium (DMEM; Gibco, Grand Island, NY, USA) supplemented with 10% fetal bovine serum (FBS; Procell) and 5% CO₂. All cell lines were validated by short tandem repeat (STR) analysis, and mycoplasma testing was negative.



2.4 Cell Proliferation Assay

The Cell Counting Kit-8 (CCK-8) assay (Dojindo, Kumamoto, Japan) was performed to assess proliferative potential. Cells (3 \times 10³) were seeded in 96-well plates and cultured for 0, 24, 48, 72, and 96 h. Absorbance was recorded at 450 nm using microplate reader (Thermo Fisher Scientific, Waltham, MA, USA) after 2-h incubating with 10 μ L CCK-8. Three independent experiments were performed.

2.5 Cell Transfection and RNA Interference

Lentiviral vectors containing short hairpin RNA (shRNA) and the *NAT10* coding sequence were purchased from Genechem (Shanghai, China). ShRNA sequence for *NAT10* was: AGGGCCCTCCTTTCCTATAAG. HeLa and SiHa cells were infected with lentivirus. Small interfering RNA (siRNA; KeScience, Shanghai, China) was utilized to knock out *NAT10* in cells using Lipofectamine 3000 (Invitrogen, Waltham, MA, USA). The siRNA sequence was: GCUGUGGUGUUAUAAGAAATT.

2.6 Cell Migration and Cell Invasion

Cell monolayer was scratched using a pipette tip, and wound width at 0, 24 h was captured using the DMC4500 digital microscope (Leica, Wetzlar, Germany). Migration distance was evaluated by ImageJ software (version 1.53t, National Institutes of Health [NIH], Bethesda, Rockville, MD, USA).

Transwell assays were performed with 8 µm chambers (Falcon; Corning Inc., Corning, NY, USA). 5×10^4 cells were suspended in DMEM containing 2% FBS and added to upper chambers. Lower chambers were filled with 20% FBS-DMEM. Remodelin (Selleck Chemicals, Shanghai, China) or dimethyl sulfoxide (DMSO; Sigma, St. Louis, MO, USA) was added to the upper chambers. For invasion assay, each insert was coated with 50 µL diluted Matrigel (BD Biosciences, Franklin Lakes, NJ, USA). After a 48-h incubation, unmigrated cells on inner surface of upper chambers were removed with cotton swabs. Upper chambers were fixed in 4% paraformaldehyde (Biosharp, Hefei, China) and stained with 0.1% methylene blue (Solarbio, Beijing, China) for 30 min. Images were captured and analyzed using ImageJ software (NIH). Three independent experiments were performed.

2.7 Western Blot

Total cell proteins were extracted, resolved by sodium dodecyl polyacrylamide gel electrophoresis (EpiZyme, Cambridge, MA, USA), and transferred electrophoretically to polyvinylidene fluoride (PVDF) membranes (Millipore-Sigma, Burlington, USA). Then PVDF membranes were blocked in rapid sealing fluid (NCM Biotech, Suzhou, China), cut by predicted molecular weight, and incubated overnight at 4 °C with NAT10 monoclonal antibody or polyclonal antibodies against SCL7A5 (1:1000, 28670-1-AP;

Proteintech, Chicago, IL, USA), vimentin (1:1000, 10366-1-AP; Proteintech), N-cadherin (1:1000, YT2988; Immunoway, Plano, TX, USA), GAPDH (1:20,000; AP0063; Bioworld, Minneapolis, MN, USA), and tubulin (1:30,000, AP0064; Bioworld, Irving, TX, USA). After washing, membranes were incubated at room temperature for 120 min with horseradish peroxidase (HRP)-conjugated goat anti-rabbit secondary antibody (1:5000, AP0063; Bioworld) or HRP-conjugated anti-mouse secondary antibody (1:5000, SA00001-1; Proteintech). The Tanon 5200 Chemiluminescent Imaging System (ChampChemi 610; Sage Creation, Beijing, China) was used for immunoblot analysis. The original images of the western blot are presented as **Supplementary Materials**.

2.8 Quantitative PCR

Total RNA was extracted using TRIzol reagent (Thermo Fisher Scientific) and reverse transcribed to cDNA using PrimeScript RT Master Mix (Yeasen Biotech, Shanghai, China). Quantitative PCR (qPCR) was performed using cDNA as the template and SYBR Premix Ex Taq (Yeasen Biotech). Data were normalized to GAPDH expression. The primers for qPCR (Generay Biotech Co., Shanghai, China) were as follows: GAPDH (forward): GGAGCGAGATCCCTCCAAAAT, GAPDH GGCTGTTGTCATACTTCTCATGG; NAT10 (reverse): ATAGCAGCCACAAACATTCGC, NAT10 (forward): (reverse): ACACACATGCCGAAGGTATTG; SCL7A5 (forward): CCGTGAACTGCTACAGCGT, SCL7A5 (reverse): CTTCCCGATCTGGACGAAGC.

2.9 RNA Sequencing and Data Analysis

We employed the phenol-chloroform method to isolate and purify the total RNA from the Siha ShNAT10 vector and its OE-NAT10 cell line. RNA-seq of the Siha ShNAT10 vector and its OE-NAT10 cell line was conducted by Guangzhou Epibiotek Co., Ltd., China. Prepare EpiTM mRNA Capture Beads (Epibiotek, cat. no. R2020-96) by balancing them at room temperature for 0.5 h. One µg RNA and Beads Binding Buffer were added to the beads, then heated at 65 °C for 5 minutes and 25 °C for another 5 minutes. After magnetically clarified with the beads, the supernatant was discarded. Tris Buffer was added and heated at 80 °C for 2 minutes. We re-added Beads Binding Buffer and repeated the heating process at 65 °C and 25 °C. After the reaction was over, the mixture was magnetically clarified, and supernatant was discarded. Beads were washed with Beads Wash Buffer, and finally, Elution Buffer was added, incubated at 95 °C for 5 minutes. Supernatant was collected, which contains the mRNA elution solution. The EpiTM mRNA Library Fast kit (Epibiotek, #R1810, Guangzhou, Chia) was used to prepare the library. The library quality with the Bioptic Qsep100 Analyzer was checked to ensure the size distribution matches theoretical expectations. Library preparation was done using the



VAHTS Stranded mRNA-seq Library Prep Kit for Illumina V2 (Vazyme Biotech, Nanjing, China, NR612-02). Reads were aligned to the GRCh38 human genome using Hisat2 aligner with the "rna-strandness RF" parameter. Feature counts were utilized to calculate reads mapped to genome, and DEGSeq R-package (version 1.44.0) was applied for differential gene expression analysis.

2.10 ac4C Dot Blot

Total RNA (5 μ g) was heated at 75 °C for 5 min and then cooled to 0 °C for 1 min. Then the membranes were loaded with Amersham Hybond-N+ (0.22 μ m, 66485; Pall Co., Port Washington, NY, USA) and crosslinked twice with ultraviolet light. After blocking membranes in 5% skim milk (BD Biosciences, Franklin Lakes, NJ, USA), they were incubated overnight at 4 °C with anti-ac4C antibody (1:1000, ab252215; Abcam, Cambridge, UK). Membranes were washed with Tris-buffered saline with Tween 20 (NCM Biotech) and incubated at room temperature with anti-rabbit secondary antibody (1:5000, AP0063; Bioworld). Proteins were detected by incubating the membranes with a chemiluminescent HRP substrate (NCM Biotech), followed by staining with methylene blue buffer (Solarbio) for 30 min.

2.11 Acetylation Site Prediction

We used the prediction of N4-acetylcytidine (ac4C) modification sites in mRNA (PACES) tool to analyze potential acetylation sites of *SLC7A5* mRNA coding sequence (http://rnanut.net/paces).

2.12 ac4C RNA Immunoprecipitation

For the ac4C RNA immunoprecipitation assay, cells were lysed using NP40 (Beyotime, Jiangsu, China) at 4 °C overnight. Twenty μL of solution was stored at –80 °C. Next, 200 μL lysate was mixed with anti-ac4C antibody (1:50, ab252215; Abcam), and another 200 μL lysate was mixed with normal rabbit IgG (1:50, 30000-0-AP; Proteintech) at 4 °C for 4 h. Protein A/G beads (MedChemExpress, Monmouth Junction, NJ, USA) were incubated with lysate at 4 °C overnight. Next morning, the beads were washed with buffer. Finally, the RNA was extracted and tested by qPCR.

2.13 mRNA Stability Assay

Actinomycin D (a transcription inhibitor) was used to evaluate RNA stability. Actinomycin D at a concentration of 200 nM was added to culture medium and co-cultured with cells as the experimental group, whereas cells cultured in complete medium served as control group. At 0, 6, and 12 h after actinomycin D treatment, cells were collected for extracting RNA. Total RNA was used for qPCR, and the level of *SLC7A5* was detected at each time point.

2.14 BALB/c Nude Mouse Xenograft Model

BALB/c nude mice have a mutation in the FOXn1 gene, which leads to the absence or degeneration of the thymus and the lack of mature T cells, making them able to accept foreign transplanted cells without producing an immune rejection response. This characteristic makes BALB/c nude mice an ideal model for studying tumor growth and metastasis. BALB/c nude mouse tumor models can retain the morphological and genetic characteristics of the primary tumor, which is of great significance for studying the biological characteristics of tumors and tumor therapy. Therefore, we selected BALB/c nude mice as a xenograft model to explore the anti-tumor effects of Remodelin in vivo. All animal experiments followed rules of the Ethics Committee on Animal Experiments of Zhujiang Hospital (Guangzhou, China). Female mice (BALB/c, 5-6 weeks old, 16-19 g; Gongsimingzi, Zhaoqing, China) were housed under pathogen-free conditions. Animal experiments were performed as previously reported [31]. Briefly, 12 mice were subcutaneously injected in the right axillary fossa with SiHa cells (2×10^6) in 100 µL phosphatebuffered saline. Ten mice developed tumors. Mice were randomized into two groups: remodelin (5 mg/kg) (Selleck) or DMSO (Sigma) vehicle (control group) administered intraperitoneally every 3 days. We measured the size of the subcutaneous transplant tumors with calipers every other day. Tumor volume (mm³) = $0.5 \times long diameter \times short$ diameter². All mice were anesthetized by intraperitoneal injection of 80 mg/kg pentobarbitone (Cat# DORMINAL 20%; Macklin, Shanghai, China. The stock concentration is 200 mg/ml, and is diluted with saline to a concentration of 16 mg/ml, and administered at 5 ml/kg to give a dose of 80 mg/kg) after almost 3 weeks of treatment and sacrificed by cervical dislocation after being photographed. Their neoplasms were dissected.

2.15 Chicken Chorioallantoic Membrane Assay

Fertilized eggs (Eggsiao, Suzhou, China) were developed for 10 days. Then they were laid on their side and the shell were punctured on the air bag side (the top side). After sucking the air from the airbag, the chicken chorioal-lantoic membranes (CAMs) were dropped. Next, $100~\mu L$ cell suspension containing 1,000,000 cells was inoculated per CAM. Tumors were collected after incubation at 37 °C in an incubator for 6 days.

2.16 Statistical Analyses

Data were analyzed using GraphPad Prism 9 software (GraphPad Software Inc., San Diego, CA, USA). Data are presented as the mean ± standard deviation. *t*-test was used to compare differences between two groups, if data followed a normal distribution. For more than three groups, one- or two-way analysis of variance followed by Bonferroni's post-hoc tests were used. If the data did not follow a normal distribution or were categorical, non-parametric



Table 1. Relationship between NAT10 expression and clinicopathological characteristics of 110 patients with cervical cancer.

Clinical parameter		Total (cases%)	NAT10 expression level		χ^2	n
Chinical parameter			High expression	Low expression	X	p
Total		110	62	48		
Age (years)	< 50	76	38 (50%)	38 (50%)	4.048	0.042
	≥50	34	24 (70.59%)	10 (29.41%)		
Histological type	Squamous cell cancer	100	56 (56%)	44 (44%)	0.137	0.934
	Adenocarcinoma	3	2 (66.67%)	1 (33.33%)		
	Others	7	4 (57.14%)	3 (42.86%)		
Pathological stage	I–II	91	52 (57.14%)	39 (42.86%)	0.13	0.72
	III–IV	19	10 (52.63%)	9 (47.37%)		
Pathological grading	I/II/I—II	14	10 (71.43%)	4 (28.57%)	0.38	0.76
	II–III/III	78	49 (62.82%)	29 (37.18%)		
Lymph node metastatic	Negative	92	52 (56.52%)	40 (43.48%)	0.0057	0.94
	Positive	18	10 (55.56%)	8 (44.44%)		
Recurrent condition	Yes	36	22 (61.11%)	14 (38.89%)	0.49	0.48
	No	74	40 (54.05%)	34 (45.95%)		

NAT10, N-acetyltransferase 10.

tests such as the Wilcoxon rank-sum test or chi-square test were applied. To ensure statistical power, each experiment was repeated three times. Survival curves were analyzed using the Kaplan–Meier method. Statistical significance was set at p < 0.05.

3. Results

3.1 NAT10 is Overexpressed in Cervical Cancer and is Correlated with Poor Prognosis

We found that NAT10 mRNA high expression was closely correlated with shorter disease-free survival (DFS) and overall survival (OS) of patients with CESC in TCGA (Fig. 1A,B). Clinical characteristics of patients were shown Supplementary Table 1. Furthermore, association between NAT10 mRNA expression and OS of patients with cervical adenocarcinoma was assessed, and high expression of NAT10 mRNA was correlated with shorter OS of patients with cervical adenocarcinoma (Supplementary Fig. 1). To further explore NAT10 expression and its association with patient prognosis, a commercial cervical cancer tissue chip was used to detect NAT10 protein levels by immunohistochemistry (IHC). The chip included 110 cervical cancer tissues and 25 adjacent non-cervical cancer tissues. Results showed NAT10 protein expression in nuclei and cytoplasm of cervical cancer cells (Fig. 1C), which was significantly higher in cervical cancer tissues than in normal ones (Fig. 1C,D). Kaplan-Meier curves revealed that patients with high NAT10 expression had lower OS and DFS (Fig. 1E,F), suggesting that NAT10 might predict poor prognosis. Interestingly, we found that NAT10 was overexpressed in older patients compared with young patients (Table 1), consistent with evidence showing involvement NAT10's involvement in age-related disorders [32]. However, we found that NAT10 was not correlated with lymph node metastasis, pathological stage, or pathological grade (Table 1).

3.2 NAT10 Potentiates Cervical Cancer Cell Proliferative and Metastatic Potentials

To evaluate NAT10's role in cervical cancer, four cervical cancer cell lines (SiHa, CaSki, C33A, and HeLa) were used to detect NAT10 expression. NAT10 was detected in all of these cell lines and was overexpressed in Caski and SiHa cells (Fig. 2A). ShNAT10 and SiNAT10 were used to repress NAT10 expression in CaSki and SiHa cells, respectively. NAT10 expression was significantly reduced after NAT10 knockdown (Fig. 2B,C). The proliferative ability of SiHa and CaSki cells was decreased after silencing NAT10 (Fig. 2D). Wound healing assays showed that NAT10 downregulation slowed wound healing in these cells (Fig. 2E). Silencing of NAT10 also decreased the migratory and invasive abilities of SiHa and CaSki cells (Fig. 2F,G). Subsequently, we found that NAT10 knockdown attenuated cervical cancer cell proliferation *in vivo* in CAMs (Fig. 2H,I).

We explored the role of NAT10 by overexpressing NAT10 in a SiHa NAT10-knockdown cell line (ShNAT10 cell line) using the lentivirus method. NAT10 expression in the SiHaShNAT10 overexpression (OE) cell line was significantly increased after transfection with OE lentivirus (Fig. 3A,B). Cell proliferative ability was significantly enhanced after NAT10 overexpression (Fig. 3C). Moreover, overexpression of NAT10 promoted wound healing in SiHa cells (Fig. 3D). NAT10 overexpression promoted SiHa cell metastasis and invasion in transwell assays (Fig. 3E,F). We also overexpressed NAT10 in HeLa cervical cancer cells. Similarly, NAT10 expression in the HeLa-NAT10 OE cell line was increased after transfection with OE lentivirus (Fig. 3A,B). Together, NAT10 overexpression promoted proliferation, wound healing, invasion, and metastasis abilities of HeLa cells (Fig. 3C-F), indicating that NAT10 is an oncogene in cervical cancer.



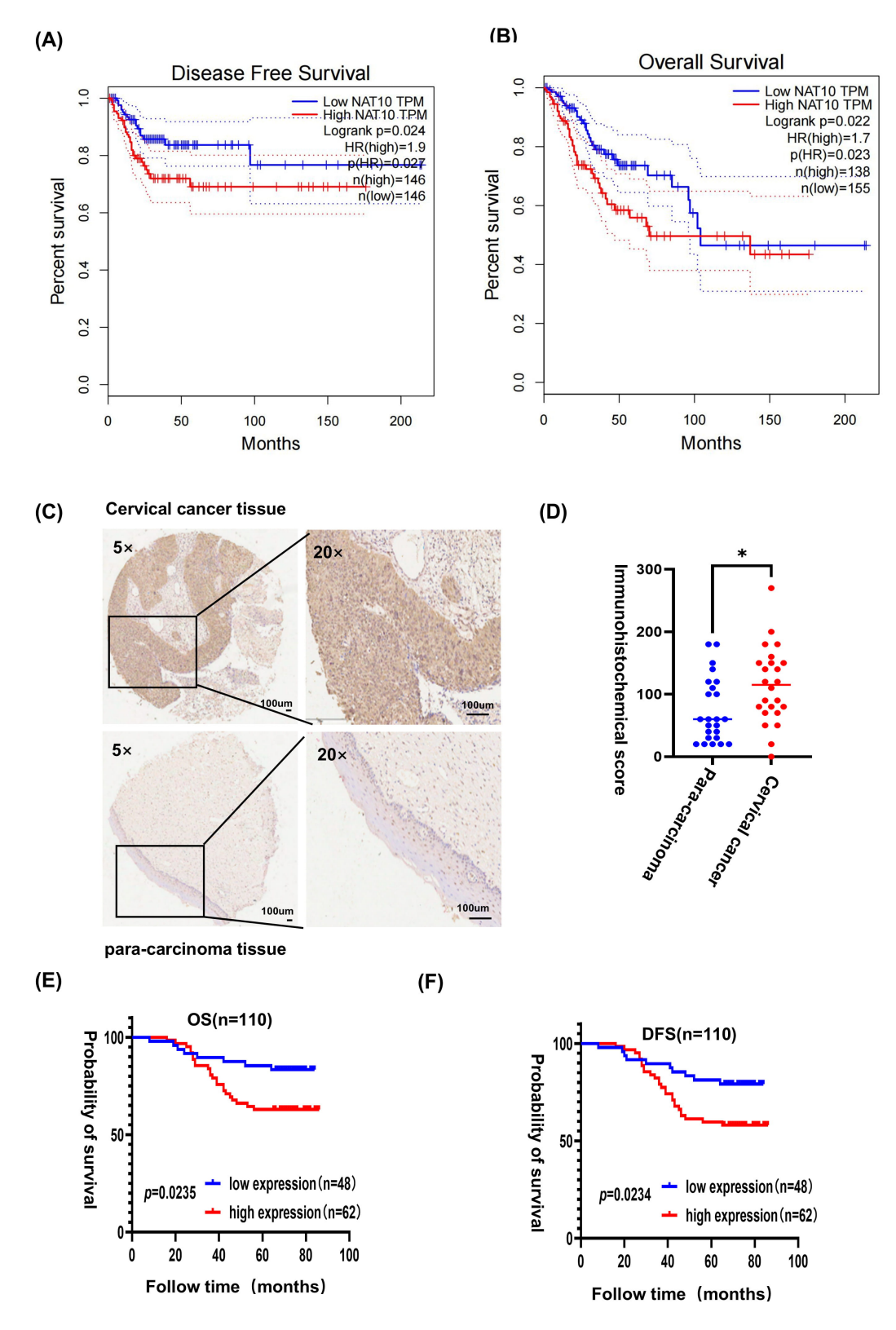


Fig. 1. NAT10 is overexpressed in cervical cancer. (A) Effect of NAT10 expression level on DFS of patients with cervical cancer based on TCGA dataset. (B) Effect of NAT10 expression level on OS of patients with cervical cancer based on TCGA dataset. (C) Representative IHC images of cervical microarrays showing NAT10 expression in cervical tumors and corresponding normal tissues. Scale bar for the images is $20 \times$, $100 \, \mu m$. (D) NAT10 expression in cervical cancer and adjacent tissues. (E) Effect of NAT10 on OS of patients with cervical cancer. (F) Effect of NAT10 on DFS of patients with cervical cancer. TGCA, the cancer genome atlas; IHC, immunohistochemistry; TPM, transcripts per million; OS, overall survival; DFS, disease-free survival; NAT10, N-acetyltransferase 10. Note: *p < 0.05.

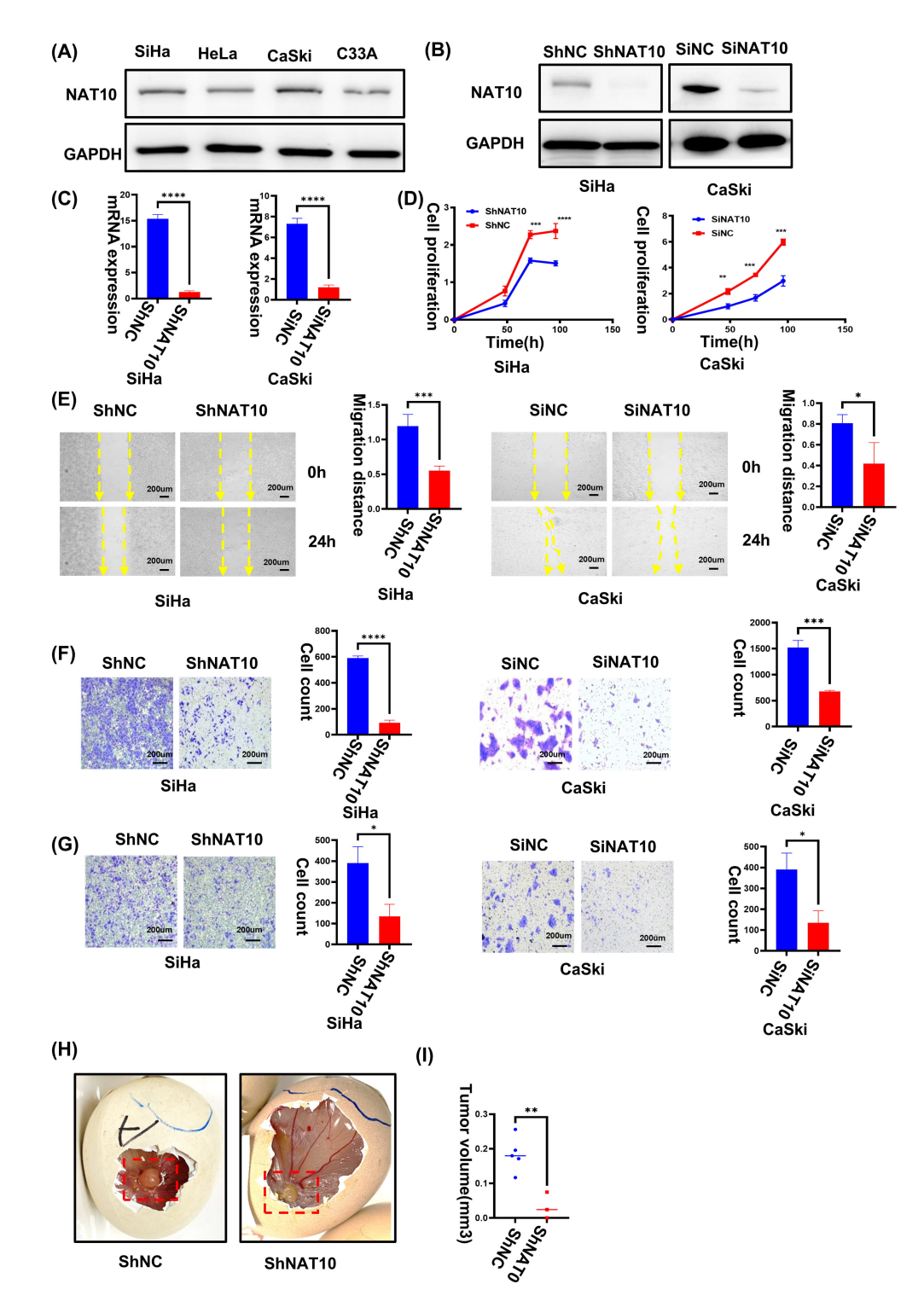


Fig. 2. Knockout of NAT10 expression impaired proliferative and metastatic potentials of cervical cancer cells. (A) Expression of NAT10 in four cervical cancer cell lines. (B) Knockdown efficiency of NAT10 determined by Western blotting. (C) Validation of NAT10 mRNA knockdown by qPCR (n = 3). (D) NAT10 silence impaired proliferative potential of SiHa (n = 4) and CaSki cells (n = 3). (E) NAT10 silence inhibited wound healing of SiHa (n = 3) and CaSki cells (n = 3). Scale bar = 200 μ m. (F) Cell migratory capacity was reduced after NAT10 knockdown) (n = 3). Scale bar = 200 μ m. (G) Knockdown of NAT10 expression reduced the invasion capability of SiHa (n = 3) and CaSki cells (n = 3). Scale bar = 200 μ m. (H) Representative images of tumors in CAMs after knockdown of NAT10 expression in SiHa cells. (I) Knockout of NAT10 expression in SiHa cells inhibited the proliferation of tumors in CAMs (n = 3–5). NAT10, N-acetyltransferase 10; ShNC, negative control short hairpin RNA; ShNAT10, short hairpin RNA targeting NAT10; SiNC, negative control small interfering RNA; SiNAT10, small interfering RNA targeting NAT10; OD, optical density; CAMs, chicken chorioallantoic membranes; qPCR, quantitative PCR. Note: *p < 0.05, **p < 0.01, ****p < 0.001, ****p < 0.0001.

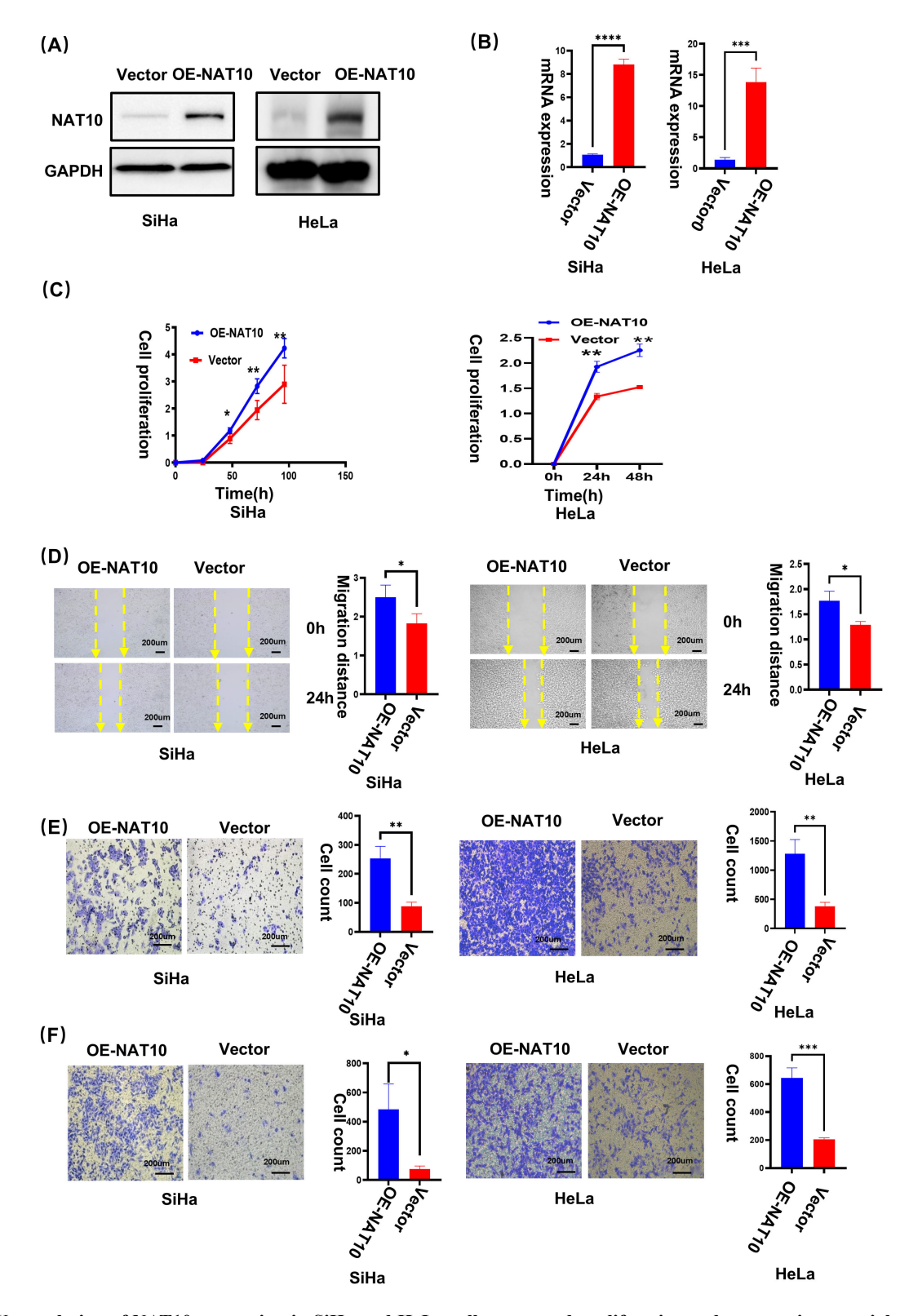


Fig. 3. Upregulation of NAT10 expression in SiHa and HeLa cells promoted proliferative and metastatic potentials of cervical cancer cells. (A) NAT10 protein overexpression as confirmed by Western blotting. (B) Determination of *NAT10* mRNA overexpression by qPCR (n = 3). (C) Promotion of cell proliferation after overexpressing NAT10 in SiHa (n = 5) and HeLa cells (n = 3). (D) Effect of NAT10 overexpression on migration of SiHa (n = 3, scale bar = 200 μ m) and HeLa cells (n = 3, scale bar = 200 μ m) was evaluated using a wound healing assay. (E) Migration capability of SiHa and HeLa cells overexpressing NAT10 as evaluated by transwell assays (n = 3, scale bar = 200 μ m). (F) Invasion capability of SiHa and HeLa cells overexpressing NAT10 as evaluated by transwell assays (n = 3, scale bar = 200 μ m). NAT10, N-acetyltransferase 10; OE-NAT10, NAT10 overexpression; OD, optical density. Note: *p < 0.05, **p < 0.01, ***p < 0.001, ****p < 0.0001.

3.3 NAT10 Regulates Progression of Cervical Cancer Cells by ac4C Acetylation

NAT10 acts as an acetyltransferase that can catalyze ac4C modification on mRNA, thereby improving mRNA stability and translation efficiency [13,17,33]. We performed an acetylation dot blot assay to investigate whether NAT10 exerts its biological effects by acetylating mRNA in cervical cancer cells. Inhibiting NAT10 in SiHa cells significantly reduced the mRNA ac4C acetylation level (Fig. 4F), consistent with previous reports [13,17]. Increased ac4C acetylation level was detected when NAT10 was overexpressed in SiHa cells (Fig. 4F).

3.4 Exploration of Downstream Factors of NAT10 in Cervical Cancer

To decipher mechanisms by which NAT10 affects cervical cancer cell progression, RNA-seq was performed on NAT10-overexpressing SiHa and control cells. The sequencing results showed that 1146 genes were upregulated and 1097 genes were downregulated after NAT10 overexpression in SiHa cells (Fig. 4A). The top 10 significantly enriched gene ontology terms are summarized in Fig. 4B. The results showed that NAT10 was related to several biological processes such as "the C21-steroid hormone metabolic process", "progesterone metabolic process", "homophilic cell adhesion via plasma membrane adhesion molecules", and "carboxylic acid transport". Kyoto encyclopedia of genes and genomes pathway enrichment analysis indicated that the differentially expressed genes were significantly enriched in "ATP-binding cassette transporters", "neuroactive ligand-receptor interactions", and "protein digestion and absorption" (Fig. 4C).

SLC7A5 upregulation is correlated with increased activity in the carboxylic acid transport and organic anion transport pathways [23]. Based on data from TCGA website, NAT10 mRNA expression was positively correlated with SLC7A5 mRNA expression (Fig. 4D). NAT10 can reportedly function by acetylating target mRNA [34]. Therefore, we consulted an acetylation site prediction website, which showed that there are acetylation sites at nucleotides 120 and 134 of SLC7A5 mRNA, with a specificity of 99% (Fig. 4E). Consequently, we speculate that SLC7A5 mRNA is a potential downstream target of NAT10.

3.5 SLC7A5 Plays a Carcinogenic Role in Cervical Cancer

By analyzing the public database, *SLC7A5* mRNA was highly expressed in cervical cancer tissues (Fig. 5A). Overexpression of *SLC7A5* was associated with a low OS rate in cervical cancer (Fig. 5B), both in squamous cell carcinoma (Fig. 5C) and adenocarcinoma (Fig. 5D). Moreover, patients with high *NAT10* and *SLC7A5* mRNA expression had worse OS than those with low levels according to bioinformatics analysis (Fig. 5E), both in squamous cell carcinoma (Fig. 5F) and adenocarcinoma (Fig. 5G). We also found that samples with overexpressed *NAT10* and

SLC7A5 had a higher degree of M2 macrophage infiltration and lower degree of M1 macrophages (Fig. 5H). Knockdown of SLC7A5 (Fig. 5I,J) in SiHa cells significantly reduced wound healing (Fig. 5K), migration, and invasion abilities (Fig. 5L).

3.6 NAT10 can ac4C Acetylate SLC7A5 mRNA and Regulate its Stability

Next, qPCR was performed for verification purposes. *SLC7A5* was significantly decreased after knockdown of NAT10 but was significantly increased after overexpression of NAT10 (Fig. 6A). Western blot analysis showed similar results (Fig. 6B). The acetylated RNA immunoprecipitation-qPCR results further showed that NAT10 downregulation in cervical cancer cell lines significantly decreased acetylation level of *SLC7A5* mRNA (Fig. 6C). The results of the mRNA stability assay showed that knocking down NAT10 expression reduced *SLC7A5* mRNA stability (Fig. 6D).

3.7 Knockdown of SLC7A5 Expression Partially Reverses the Effect of NAT10 Overexpression on Cervical Cancer Progression

We speculated that NAT10 exerts its biological function by acetylating *SLC7A5* mRNA. To further explore SLC7A5's role, we silenced SLC7A5 in cervical cancer NAT10overexpressing stable cell lines (Fig. 6E,F). The results showed that after downregulating SLC7A5, the wound healing ability, which increased by NAT10 overexpression, decreased to a certain extent (Fig. 6G). Migration capacity of cervical cancer cells was also reduced to some extent following SLC7A5 downregulation (Fig. 6H).

3.8 Remodelin Inhibits Proliferative and Metastatic Abilities of Cervical Cancer Cells in Vitro and in Vivo

Remodelin is a NAT10 inhibitor [35,36]. Thus, we used remodelin to determine if NAT10 could be used as a therapeutic target for cervical cancer. CCK-8 assays revealed that remodelin significantly attenuated SiHa, CaSki, and C33A cell proliferation (Fig. 7A). Remodelin significantly weakened the wound healing ability of Siha, CaSki, and C33A cells compared to controls (Fig. 7B–D). Remodelin decreased migratory (Fig. 7E–G) and invasive abilities of SiHa, CaSki, and C33A cells (Fig. 7H–J). These results further confirmed that NAT10 is a potential target for cervical cancer, and that remodelin is a promising therapeutic drug that might attenuate cervical cancer progression.

We found that remodelin attenuated growth and reduced the weight of cervical tumors (Fig. 8A–C). IHC showed that Ki67 expression (marker of tumor proliferation) was reduced after remodelin treatment (Fig. 8F). Western blotting showed that remodelin significantly decreased N-cadherin and vimentin levels (Fig. 8E), indicating that remodelin inhibits the epithelial–mesenchymal transition in cervical cancer tumors *in vivo*. More importantly, treatment with remodelin had little effect on organ damage in mice

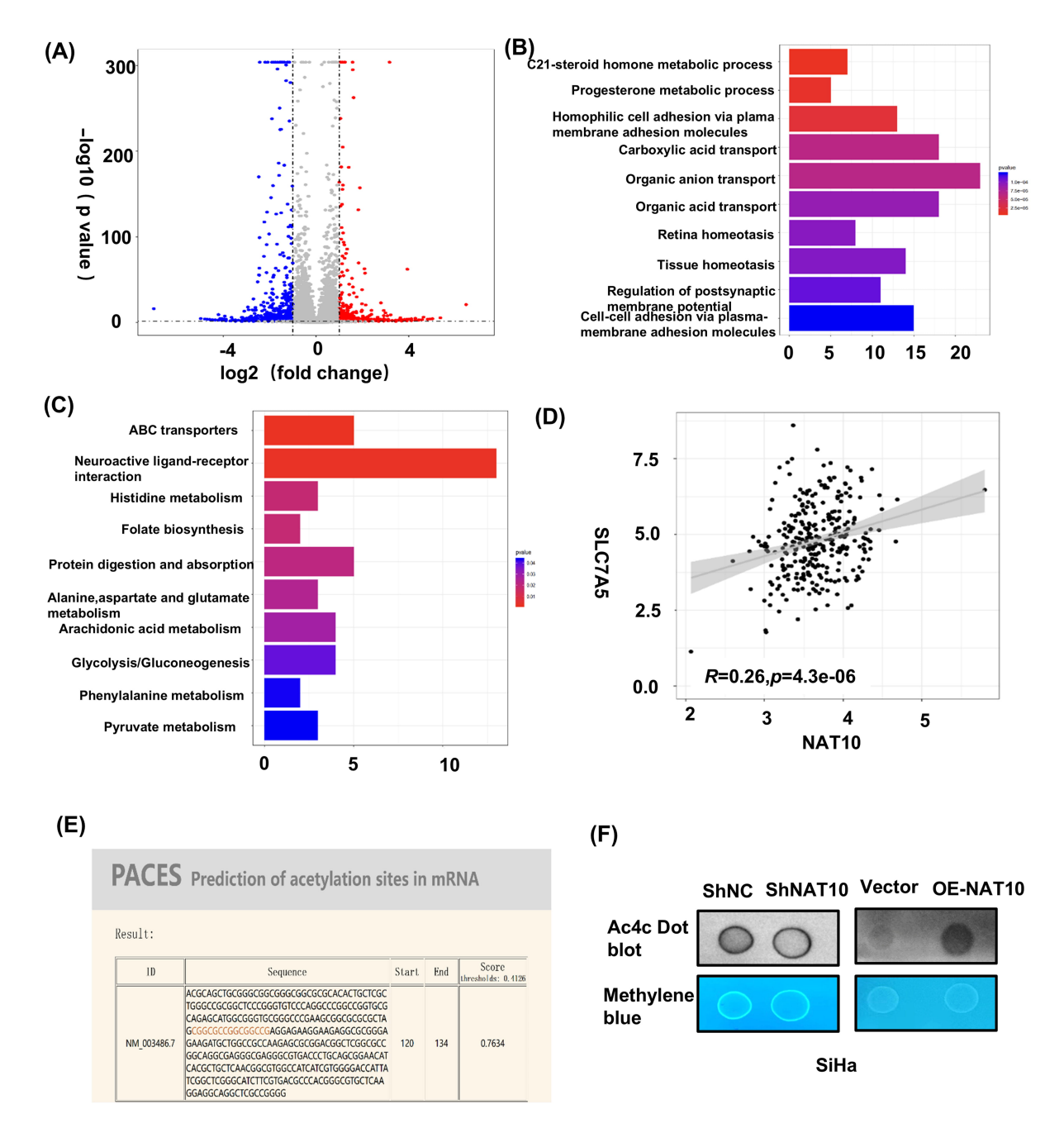


Fig. 4. Exploration of the impact of NAT10 on downstream factors. (A) Transcriptomic comparison was carried out to analyze the dysregulated genes between the vector control and OE-NAT10 (NAT10 overexpressing) SiHa cells. (B) Representative pathway analysis terms according to Gene Ontology analysis. (C) Representative pathway analysis terms according to Kyoto Encyclopedia of Genes and Genome analysis. (D) Scatter plot of TPM values of NAT10 and SLC7A5 mRNA in TCGA-CESC data. Spearman's correlation analysis showed the association between NAT10 mRNA and SLC7A5 mRNA expression levels (log2 [TPM + 1]) (R = 0.26, $p = 4.3 \times 10^{-6}$). (E) Prediction conserved acetylation sites in the SLC7A5 coding sequence in PACES tools (http://rnanut.net/paces/). (F) Detection of ac4C acetylation on mRNA of cervical cancer cells using an ac4C dot blot assay. NAT10, N-acetyltransferase 10; SLC7A5, solute carrier family 7 member 5; TPM, transcripts per million; TCGA, the cancer genome atlas; CESC, cervical squamous cell carcinoma; ac4C, N4-acetylcytidine; PACES, prediction of N4-acetylcytidine (ac4C) modification sites in mRNA.

(Fig. 8G), indicating its safety. SLC7A5 expression was reduced after remodelin treatment *in vivo* by qPCR and IHC (Fig. 8D,F).

4. Discussion

NAT10 is a member of epigenetic modifications and exerts essential functions in cancer development. Here, we confirmed that NAT10 is overexpressed in cervical can-



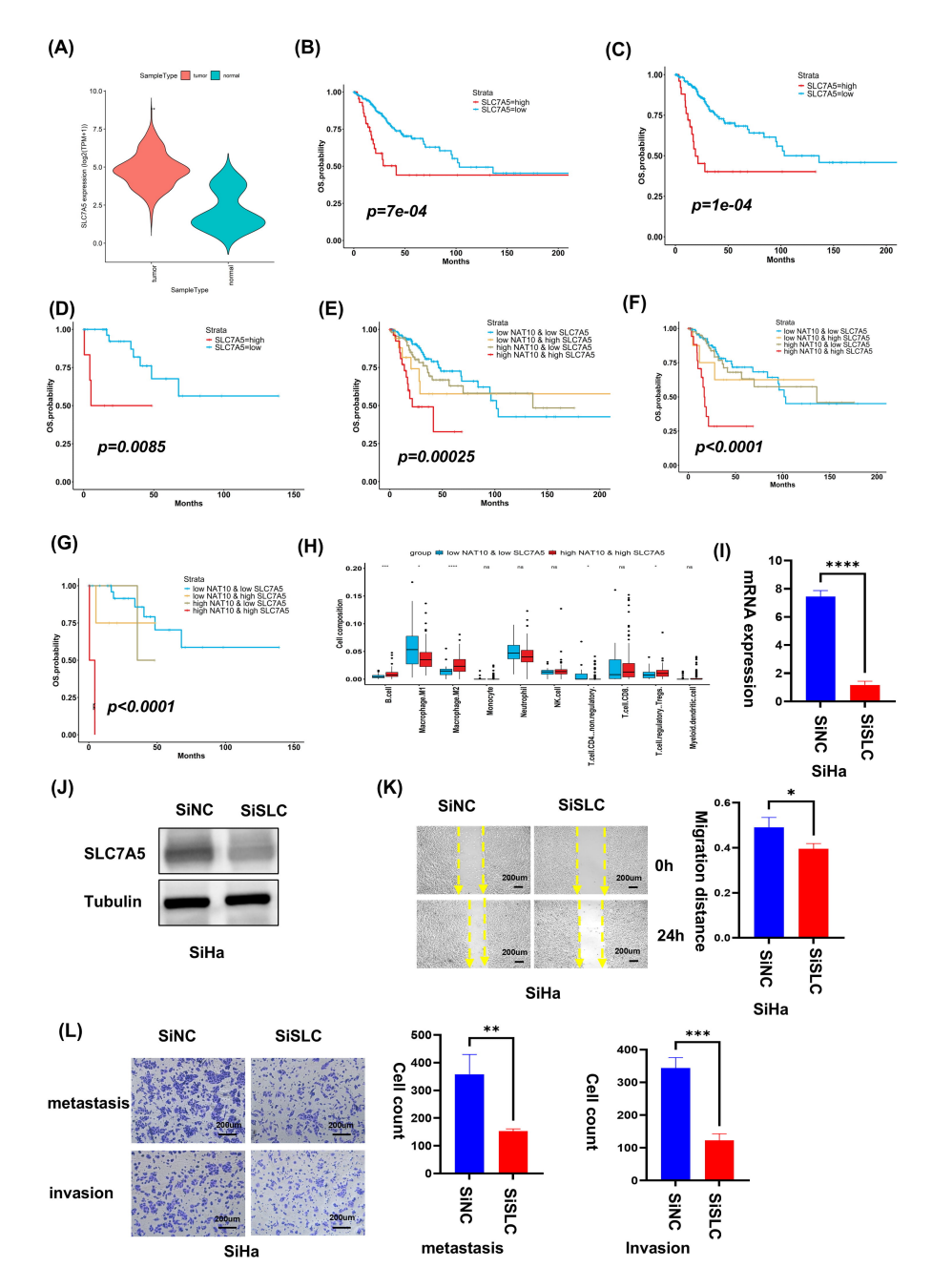


Fig. 5. SLC7A5 is a carcinogenic factor in cervical cancer. (A) SLC7A5 mRNA was overexpressed in cervical cancer compared with normal cervical tissue. (B) Overexpression of SLC7A5 mRNA corelated with poor OS in cervical cancer. (C) Overexpression of SLC7A5 mRNA corelated with poor OS in squamous cell carcinoma of the cervix. (D) Overexpression of SLC7A5 mRNA corelated with poor OS in cervical adenocarcinoma. (E) Patients with high NAT10 and SLC7A5 mRNA expression had worse OS than those with low levels according to bioinformatics analysis. (F) Patients with high NAT10 and SLC7A5 mRNA expression in cervical squamous cell carcinoma had worse OS than those with low levels according to bioinformatics analysis. (G) Patients with high NAT10 and SLC7A5 mRNA expression in cervical adenocarcinoma had worse OS than those with low levels according to bioinformatics analysis. (H) Differences in abundance of 10 immune cell types enriched in the TCGA-CESC dataset based on quanTIseq algorithm; blue indicates the "low NAT10 & low SLC7A5" group, red indicates the "high NAT10 & high SLC7A5" group; the horizontal axis indicates the 10 immune cell types, and the vertical axis the abundance of immune cell infiltration. (I) Validation of SLC7A5 mRNA knockdown level by qPCR in SiHa cells (n = 3). (J) Knockdown efficiency of SLC7A5 determined by Western blotting in SiHa cells. (K) Knockdown of SLC7A5 expression inhibited the wound healing of SiHa cells (n = 3, scale bar = 200 μ m). (L) Cell migratory and invasive capacities of SiHa cells were reduced after SLC7A5 knockdown (n = 3, scale bar = 200 μ m). OS, overall survival; NAT10, N-acetyltransferase 10; SLC7A5, solute carrier family 7 member 5; TCGA-CESC, the cancer genome atlas cervical squamous cell carcinoma and endocervical adenocarcinoma; qPCR, quantitative PCR; ns, not significant. Note: p < 0.05; **p < 0.01; ***p < 0.001; ****p < 0.001.



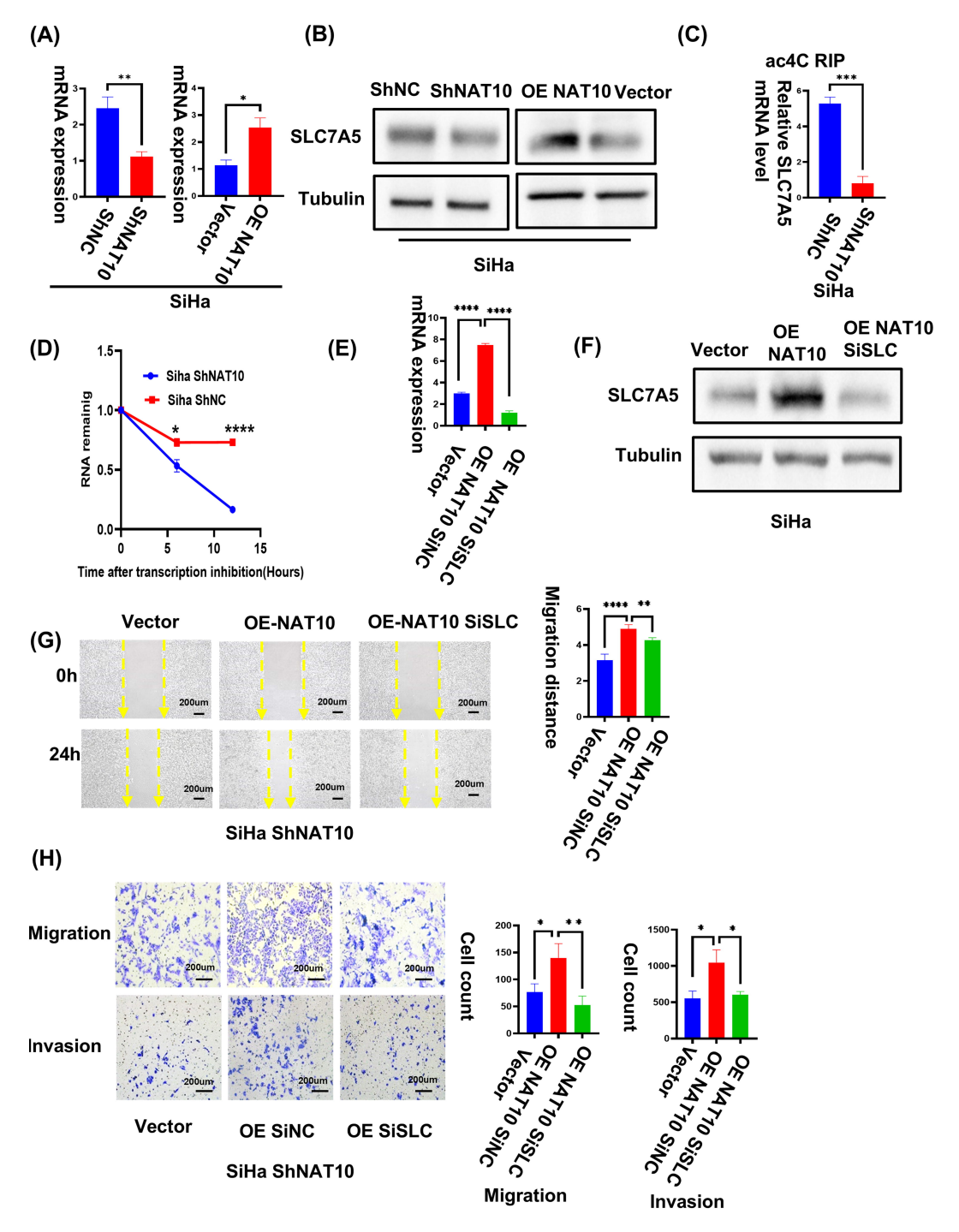


Fig. 6. NAT10 affected the biological behavior of cervical cancer cells by ac4C acetylation of SLC7A5 mRNA. (A) Validation of the mRNA level of SLC7A5 by qPCR after regulating NAT10 expression (n = 3). (B) Detection of SLC7A5 protein levels by western blotting after regulating NAT10 expression in cervical cancer cells. (C) Detection of SLC7A5 mRNA level by acetylated RNA immunoprecipitation-qPCR after knocking down NAT10 in SiHa cells (n = 3). (D) Reducing NAT10 expression in SiHa decreased the stability of SLC7A5 mRNA (n = 3). (E) Determination of the knockout efficiency of SLC7A5 mRNA by qPCR in SiHa OE NAT10 cell lines (n = 3). (F) Determination of the knockout efficiency of SLC7A5 by western blotting in SiHa OE NAT10 cell lines. (G) The cell migration capability, which increased by NAT10 overexpression, decreased to a certain extent after SLC7A5 knockdown, as determined by wound healing assays (n = 3, scale bar = SLC7A5 by transwell assays (n = 3, scale bar = SLC7A5 knockdown, as determined by wound healing assays (n = 3, scale bar = SLC7A5 by transwell assays (n = 3, scale bar = SLC7A5 knockdown, as determined by wound healing assays (n = 3, scale bar = SLC7A5 knockdown, as determined by wound healing assays (n = 3, scale bar = SLC7A5 knockdown, as determined by wound healing assays (n = 3, scale bar = SLC7A5 knockdown, as determined by wound healing assays (n = 3, scale bar = SLC7A5 knockdown, as determined by wound healing assays (n = 3, scale bar = SLC7A5 knockdown, as determined by wound healing assays (n = 3, scale bar = SLC7A5 knockdown, as determined by wound healing assays (n = 3, scale bar = SLC7A5 knockdown, as determined by wound healing assays (n = 3, scale bar = SLC7A5 knockdown, as determined by wound healing assays (n = 3, scale bar = SLC7A5 knockdown, as determined by wound healing assays (n = 3, scale bar = SLC7A5 knockdown, as determined by wound healing assays (n = 3, scale bar = SLC7A5 knockdown, as determined by wound healing assays (n = 3

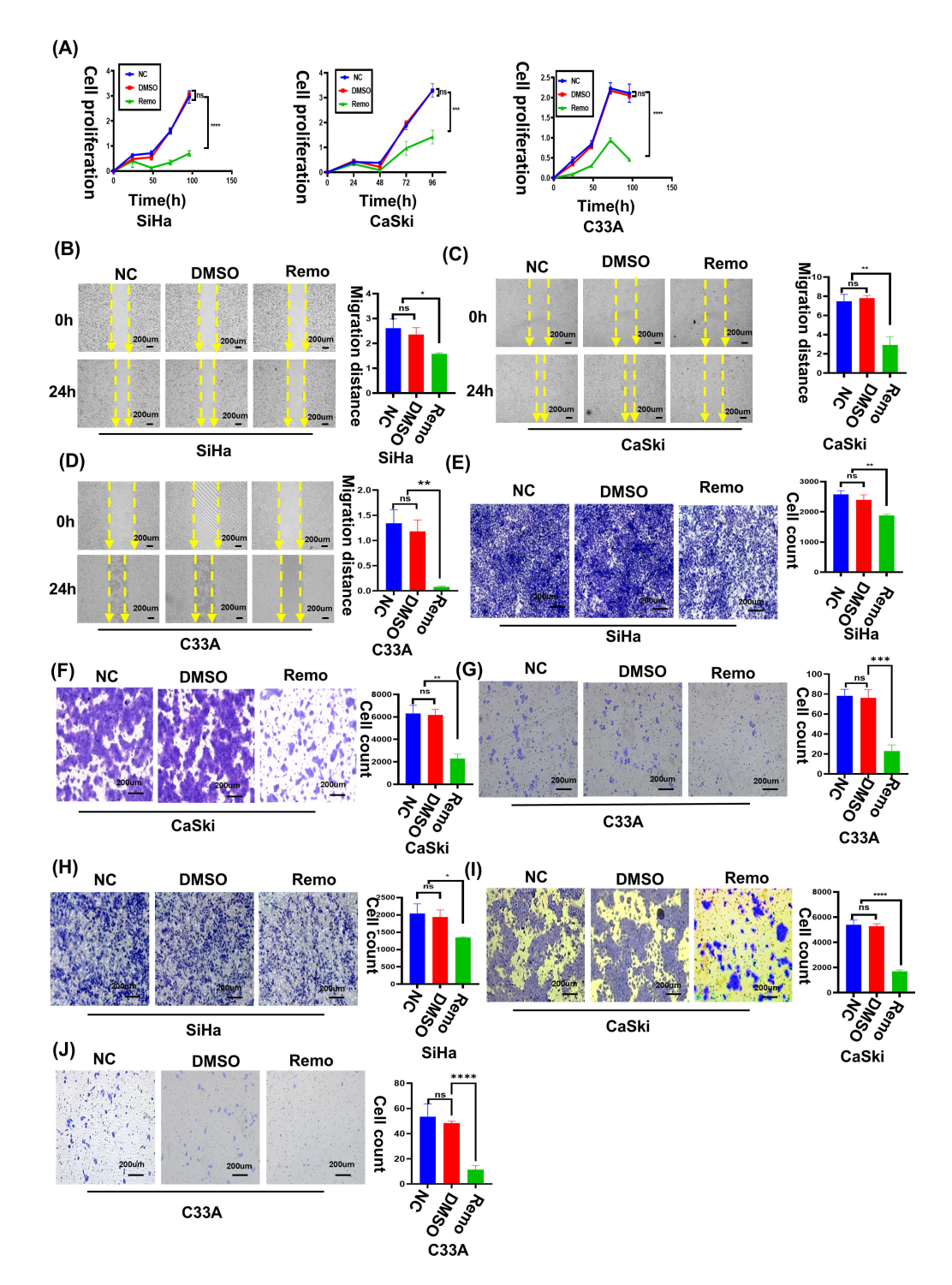


Fig. 7. Remodelin, inhibitor of NAT10, impaired proliferative and mestatic potentials of cervical cancer cells. (A) Remodelin impaired proliferation of cervical cancer cells (SiHa, CaSki, and C33A) as shown by CCK-8 assays (n = 3). (B) Remodelin impaired the migration capability of SiHa cells by wound healing assays (n = 3, scale bar = 200 μ m). (C) Remodelin impaired the migration capability of CaSki cells as shown by wound healing assays (n = 3, scale bar = 200 μ m). (E) Remodelin impaired the migration capability of SiHa cells as shown by transwell assays (n = 3, scale bar = 200 μ m). (F) Remodelin impaired the migration capability of CaSki cells as shown by transwell assays (n = 3, scale bar = 200 μ m). (G) Remodelin impaired the migration capability of C33A cells as shown by transwell assays (n = 3, scale bar = 200 μ m). (H) Remodelin impaired the invasion capability of SiHa cells as shown by transwell assays (n = 3, scale bar = 200 μ m). (I) Remodelin impaired the invasion capability of CaSki cells as shown by transwell assays (n = 3, scale bar = 200 μ m). (J) Remodelin impaired the invasion capability of CaSki cells as shown by transwell assays (n = 3, scale bar = 200 μ m). (CK-8, cell counting kit-8; NAT10, N-acetyltransferase 10. Note: *p < 0.05, **p < 0.01, ***p < 0.001, ****p < 0.0001, ns, not significant.

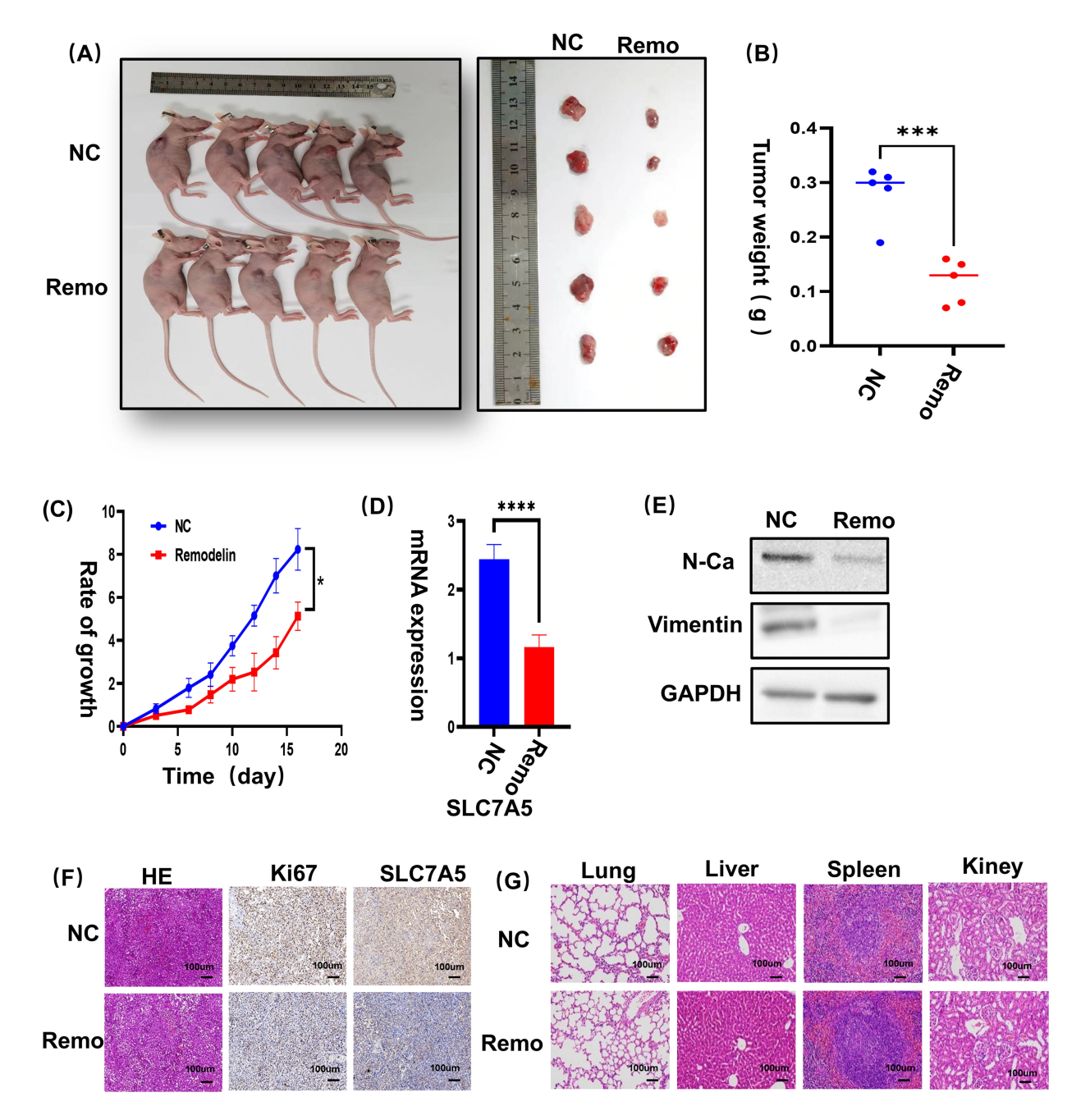


Fig. 8. Remodelin prevented cervical cancer growth in vivo. (A) Tumor images of a xenograft nude mouse model subcutaneously injected with SiHa cells and treated with remodelin or NC. (B) Weight of tumors in the remodelin and NC groups at the experiment endpoint. (C) Growth rate of the tumors with or without remodelin treatment. (D) Validation of *SLC7A5* mRNA levels in samples with or without remodelin treatment. (E) Expression of vimentin and N-cadherin after treatment with remodelin or NC as assessed by Western blotting. (F) Representative images for H&E and IHC staining of the Ki-67 (marker of proliferation) and SLC7A5 in nude mouse sections. Scale bar = $20 \times$, $100 \, \mu m$. (G) Representative H&E images of lung/liver/spleen/kidney from mice treated with remodelin or from the NC group. Scale bar is $20 \times$, $100 \, \mu m$. H&E, hematoxylin and eosin; IHC, immunohistochemistry; SLC7A5, solute carrier family 7 member 5; NC, negative control; Note: n = 5, *p < 0.05, ***p < 0.001, ****p < 0.0001.

cer, which predicted poor DFS and OS. Functionally, we showed that NAT10 plays an oncogenic role by promoting their proliferation and migration. By this mechanism, NAT10 induces the ac4C acetylation of mRNA in cervical cancer cells. We further showed that NAT10 N4-acetylates *SLC7A5* mRNA and enhances its mRNA stability in cer-

vical cancer, thus positively regulating the expression of SLC7A5. Remodelin may serve as a promising targeted agent by inhibiting cervical cancer progression both *in vitro* and *in vivo*.

Through mRNA-seq analysis, SLC7A5 mRNA was upregulated in cervical cancer cells after overexpression of



NAT10. We further found that *SLC7A5* and *NAT10* mRNA levels were closely related in cervical cancer, indicating that *NAT10* and *SLC7A5* might have a mutual regulatory relationship. An acetylation site on *SLC7A5* mRNA was predicted to have a probability of 0.76. Based on this, we hypothesize that *SLC7A5* mRNA may be a downstream target of NAT10. Through analysis of public databases, we found that *SLC7A5* mRNA is overexpressed in cervical cancer tissues and is a predictor of poor OS in cervical cancer. Patients with high *NAT10* and *SLC7A5* mRNA expression had the lowest OS. By downregulating SLC7A5 in SiHa cervical cancer cells, it can inhibit migratory and invasive abilities.

We investigated the relevant mechanisms of NAT10 and SLC7A5 in cervical cancer. The results of qPCR and Western blotting confirmed that NAT10 positively Further, ac4C RNA regulated SLC7A5 expression. immunoprecipitation-qPCR analysis revealed that NAT10 silence reduced SLC7A5 mRNA acetylation, indicating that SLC7A5 mRNA is an ac4C target of NAT10. Through RNA stability experiments, silencing NAT10 in cervical cancer cells reduced SLC7A5 mRNA stability. Together, these results showed that NAT10 can induce ac4C modification of SLC7A5 mRNA, thereby enhancing its mRNA stability and positively regulating the expression of SLC7A5. Furthermore, by knocking down the expression of SLC7A5 in cervical cancer NAT10overexpressing stable cell lines, we found that the wound healing, migration, and invasion abilities, which were increased by NAT10 overexpression, decreased to a certain extent. NAT10 can induce ac4C modification of SLC7A5 mRNA, enhance its mRNA stability, and promote SLC7A5 expression, thereby promoting the metastasis of cervical cancer. However, contrary to expectations, the proliferative ability of cervical cancer cells enhanced by NAT10 overexpression was not reduced after SCL7A5 knockdown. We speculated that other ac4C targets might exist to promote the proliferative ability of cells. Indeed, Nat10-mediated modification of mRNA acetylation is a complex biological process involving multiple molecular mechanisms and possible cofactors or cellular conditions. NAT10 is the only known enzyme that catalyzes ATP-dependent RNA acetylation to form ac4C [37]. It belongs to G-protein subunit alpha transducing protein superfamily of N-acetyltransferases and catalyzes the acetylation of histone and non-histone proteins [38]. Cofactors required for ac4C formation in mRNA have not been identified. The expression and activity of NAT10 may be regulated by a variety of transcription factors. In addition, NAT10 activity may be affected by cell energy state. For example, deacetylase sirtuin 1 was found to promote the shift of NAT10 from ribosomal RNA biosynthesis to autophagy, suggesting that the function of NAT10 may change under conditions of energy stress [15,38]. In summary, NAT10-mediated mRNA acetylation modification is a complex process involving multiple molecular levels and cellular conditions, and its specific mechanisms and influencing factors are still being studied and discovered.

According to the literature, NAT10 facilitates the acetylation of ac4C to affect the stability and translation efficiency of mRNA, thus playing a role in cervical cancer. Specifically, NAT10 can stimulate the ac4C modification of forkhead box protein P1 (FOXP1) mRNA to enhance its translation efficiency, leading to the induction of glucose transporter 4 and ketohexokinase, which are related to glycolysis metabolism. The active NAT10/ac4C/FOXP1 axis results in increased glycolysis and sustained lactate secretion in cervical cancer cells, amplifying immunosuppressive characteristics of tumor-infiltrating regulatory T cells (Tregs) in lactate-rich tumor microenvironment (TME) [39]. Another study demonstrated that NAT10's target in cervical cancer is heterogeneous nuclear ribonucleoprotein U-like 1 (HNRNPUL1). NAT10 regulates HNRNPUL1 expression in cervical cancer cells by catalyzing ac4C formation and increasing HNRNPUL1 mRNA stability [40]. Our study reveals the novel regulatory mechanism of NAT10-SLC7A5 axis in cervical cancer cells. Based on quanTIseq algorithm, there were more B cells, M2 macrophages and Tregs in tumor tissues of "high NAT10 & high SLC7A5", and less M1 macrophages. M2 macrophages appear to contribute to cancer initiation and malignant progression and immune suppression [41], whereas M1 macrophages can phagocytose tumor cells and plays a role in antitumor [42]. Consistent with previous research, we found that samples with high NAT10 expression and SLC7A5 had higher degree of M2 macrophages infiltration and lower degree of M1 macrophages. B cells in the TME may exert key functions in immunotherapy [43]. B cell-derived metabolites such as gamma-aminobutyric acid [44] and adenosine [45] have been shown to suppress the immune response against cancer. We suspect that elevated B cells in the "high NAT10 & high SLC7A5" group contribute to tumor development by suppressing anti-tumor immunity. Tregs are a doubleedged sword as they regulate immune homeostasis and inhibit cancer immune responses [46]; thus, the function of elevated Tregs in the "high NAT10 & high SLC7A5" group needs further exploration. Accordingly, we hypothesize that NAT10 may affect the expression of SLC7A5, and that SLC7A5 may play a pro-cancer role by regulating the TME, which still needs further investigation.

Remodelin, a NAT10 inhibitor, was used to decipher NAT10's therapeutic potential in cervical cancer. Our results showed that remodelin effectively inhibited progression of cervical cancer cells *in vitro* and inhibited the growth of cervical cancer cells *in vivo*. We also found that remodelin functions independently of NAT10 protein levels. Our results showed that remodelin acted as a tumor suppressor even in C33A cells with low NAT10 expression, possibly because remodelin acts by blocking the action of the lysine acetyltransferase activity of NAT10 according to the literature [18]. Nat10-targeted therapy, especially the use of re-



modelin, has shown potential clinical significance and therapeutic potential in the treatment of cervical cancer. However, more studies are needed to validate these findings and further explore the specific mechanisms and efficacy of remodelin in cervical cancer treatment.

Our study has demonstrated that NAT10 promotes cervical cancer progression through the acetylation of SLC7A5 mRNA, offering valuable insights for ongoing and future clinical trials in the fields of metabolic diseases and cancer treatment. NAT10 is upregulated in cervical cancer tissues and correlates with poor prognosis. Consequently, the expression level of NAT10 may serve as a biomarker to predict the prognosis of cervical cancer patients, aiding clinicians in developing personalized treatment plans. Additionally, this finding indicates that NAT10 could be a potential therapeutic target, and inhibiting its activity or the acetylation it mediates may suppress cervical cancer progression. As a key enzyme in mRNA acetylation, NAT10 opens new avenues for drug development in the context of cervical cancer. Future research could focus on developing small molecule inhibitors (like remodelin) or RNA interference (RNAi) technologies to block the oncogenic role of NAT10 in cervical cancer. The promotion of cervical cancer progression by NAT10 through the acetylation of SLC7A5 mRNA underscores the critical role of amino acid metabolism in tumor development. This suggests that future clinical trials should investigate inhibitors of tumor metabolic pathways, such as the glutamine metabolism inhibitor JPH203, to enhance the efficacy of tumor therapy. Bioinformatics analysis further suggests that the acetylation of SLC7A5 mediated by NAT10 may influence the tumor microenvironment, promoting cervical cancer progression. This provides scientific evidence for future clinical trials to explore strategies to improve the tumor microenvironment and enhance immune responses.

This study had some limitations. The research tools used in the study were mainly mature cervical cancer cell lines. Although they were all identified by STR and mycoplasma detection, cultured cells may undergo dedifferentiation and selection, causing cells to lose some of their biological characteristics of the original cells and affecting the accuracy of the research results. In addition, the in vitro culture environment is not completely the same as in vivo, especially the lack of regulation by the nervous and endocrine systems, which may cause changes in cell metabolism and function. In the study, we adopted strict simulation of in vivo environmental conditions, (e.g., controlling the number of passages of tumor cells) to reduce the degree of dedifferentiation of cervical cancer cells. We confirmed the role of remodelin in vivo through nude mouse experiments. Future experiments should use patient-derived tumor xenograft models to study mechanisms of NAT10 in cervical cancer and establish a more accurate and reliable experimental platform for tumor research and drug development.

5. Conclusions

In summary, we confirmed that high NAT10 expression is a poor prognostic indicator of cervical cancer and NAT10 expression affects cervical cancer cell progression. Furthermore, NAT10 potentiates proliferative and metastatic potentials of cervical cancer cells via ac4C acetylation of *SCL7A5* mRNA. Remodelin is a promising therapeutic agent for inhibiting progression of cervical cancer cells.

Availability of Data and Materials

Public gene expression data and full clinical annotations of cervical squamous cell carcinoma and endocervical adenocarcinoma (CESC) were retrieved from The Cancer Genome Atlas (TCGA) (https://portal.gdc.cancer.gov/). RNA-Seq data of the Siha ShNAT10 vector and its OENAT10 cell lines were uploaded to NCBI with ID SUB 13813349. The details of the data used in this study can be obtained from the corresponding author.

Author Contributions

YW: Conceptualization, Investigation, Supervision, Project administration and Review & Editing; XS: Conceptualization, Investigation, Supervision, Funding acquisition and Review & Editing; PL: Conceptualization, Methodology, Formal analysis, Investigation, Data Curation and Writing—Original Draft; DZ: Investigation, Resources and Data Curation; JL: Software, Validation and Formal analysis; WL: Software, Writing—Reviewing and Editing. All authors have approved the final version to be published; All authors have participated sufficiently in the work and agreed to be accountable for all aspects of the work. All authors contributed to editorial changes in the manuscript.

Ethics Approval and Consent to Participate

The animal study was conducted in accordance with the Guide for the Care and Use of the Animal Ethics Committee of Zhujiang Hospital (Guangzhou, China). The registration No. in this study was LAEC-2022-103. The animal research has followed the ARRIVE guidelines. Cervical cancer tissue microarray study was approved by the Ethics Committee of Shanghai Outdo Biotech Co., Ltd., (No. SHYJS-CP-1801014). The study was carried out in accordance with the guidelines of the Declaration of Helsinki. Informed consent was obtained from the patients or their families/legal guardians.

Acknowledgment

Thanks to all the peer reviewers for their comments and suggestions. We extend our thanks to Zhang Bingzhong for generously donating to us C33A and HeLa cell lines.



Funding

This project is supported by Guangzhou Municipal Health Science and Technology General Guidance Project (No. 20251A010068), Science and Technology Foundation of Linzhi City (SYQ2024-09), Guangzhou University-Enterprise Joint Funds (High-Level University) for Basic Research (2023A03J0375), Guangzhou University-Enterprise Joint Funds for Basic and Applied Basic Research (2024A03J0182), Guangzhou Municipal Health Science and Technology General Guidance Project (No. 20241A010068), Guangzhou City science and technology plan project (20220101465).

Conflict of Interest

The authors declare no conflict of interest.

Supplementary Material

Supplementary material associated with this article can be found, in the online version, at https://doi.org/10.31083/FBL26756.

References

- [1] Jafarinezhad S, Assaran Darban R, Javid H, Hashemy SI. The SP/NK1R system promotes the proliferation of breast cancer cells through NF-κB-mediated inflammatory responses. Cell Biochemistry and Biophysics. 2023; 81: 787–794. https://doi. org/10.1007/s12013-023-01171-y.
- [2] Vargas-Sierra O, Hernández-Juárez J, Uc-Uc PY, Herrera LA, Domínguez-Gómez G, Gariglio P, et al. Role of SLC5A8 as a Tumor Suppressor in Cervical Cancer. Frontiers in Bioscience (Landmark edition). 2024; 29: 16. https://doi.org/10.31083/j.fb 12901016.
- [3] Li C, Li Q, Li L, Sun S, Lei X. The Prognostic and Immune Significance of BZW2 in Pan-Cancer and its Relationship with Proliferation and Apoptosis of Cervical Cancer. Frontiers in Bioscience (Landmark Edition). 2024; 29: 97. https://doi.org/10.31083/j.fbl2903097.
- [4] Sung H, Ferlay J, Siegel RL, Laversanne M, Soerjomataram I, Jemal A, et al. Global Cancer Statistics 2020: GLOBOCAN Estimates of Incidence and Mortality Worldwide for 36 Cancers in 185 Countries. CA: A Cancer Journal for Clinicians. 2021; 71: 209–249. https://doi.org/10.3322/caac.21660.
- [5] Gao F, Li P, Kong X, Song T, Han Q, Zhou S. ARID1A-mutated cervical cancer depends on the activation of YAP signaling. Frontiers in Bioscience (Landmark Edition). 2021; 26: 1411– 1421. https://doi.org/10.52586/5035.
- [6] Marret G, Borcoman E, Le Tourneau C. Pembrolizumab for the treatment of cervical cancer. Expert Opinion on Biological Therapy. 2019; 19: 871–877. https://doi.org/10.1080/14712598. 2019.1646721.
- [7] Penson RT, Huang HQ, Wenzel LB, Monk BJ, Stockman S, Long HJ, 3rd, et al. Bevacizumab for advanced cervical cancer: patient-reported outcomes of a randomised, phase 3 trial (NRG Oncology-Gynecologic Oncology Group protocol 240). The Lancet. Oncology. 2015; 16: 301–311. https://doi.org/10. 1016/S1470-2045(15)70004-5.
- [8] Grau-Bejar JF, Garcia-Duran C, Garcia-Illescas D, Mirallas O, Oaknin A. Advances in immunotherapy for cervical cancer. Therapeutic Advances in Medical Oncology. 2023; 15: 17588359231163836. https://doi.org/10.1177/17588359231163836.

- [9] O'Malley DM, Neffa M, Monk BJ, Melkadze T, Huang M, Kryzhanivska A, et al. Dual PD-1 and CTLA-4 Checkpoint Blockade Using Balstilimab and Zalifrelimab Combination as Second-Line Treatment for Advanced Cervical Cancer: An Open-Label Phase II Study. Journal of Clinical Oncology. 2022; 40: 762–771. https://doi.org/10.1200/JCO.21.02067.
- [10] Schiffers S, Oberdoerffer S. ac4C: a fragile modification with stabilizing functions in RNA metabolism. RNA. 2024; 30: 583– 594. https://doi.org/10.1261/rna.079948.124.
- [11] Macinga DR, Rather PN. The chromosomal 2'-N-acetyltransferase of Providencia stuartii: physiological functions and genetic regulation. Frontiers in Bioscience. 1999; 4: D132–D140. https://doi.org/10.2741/macinga.
- [12] Wei R, Cui X, Min J, Lin Z, Zhou Y, Guo M, et al. NAT10 promotes cell proliferation by acetylating CEP170 mRNA to enhance translation efficiency in multiple myeloma. Acta Pharmaceutica Sinica. B. 2022; 12: 3313–3325. https://doi.org/10.1016/j.apsb.2022.01.015.
- [13] Wang G, Zhang M, Zhang Y, Xie Y, Zou J, Zhong J, et al. NAT10-mediated mRNA N4-acetylcytidine modification promotes bladder cancer progression. Clinical and Translational Medicine. 2022; 12: e738. https://doi.org/10.1002/ctm2.738.
- [14] Liu X, Tan Y, Zhang C, Zhang Y, Zhang L, Ren P, et al. NAT10 regulates p53 activation through acetylating p53 at K120 and ubiquitinating Mdm2. EMBO Reports. 2016; 17: 349–366. https://doi.org/10.15252/embr.201540505.
- [15] Liu X, Cai S, Zhang C, Liu Z, Luo J, Xing B, et al. Deacetylation of NAT10 by Sirt1 promotes the transition from rRNA biogenesis to autophagy upon energy stress. Nucleic Acids Research. 2018; 46: 9601–9616. https://doi.org/10.1093/nar/gky777.
- [16] Wang Z, Huang Y, Lu W, Liu J, Li X, Zhu S, et al. c-myc-mediated upregulation of NAT10 facilitates tumor development via cell cycle regulation in non-small cell lung cancer. Medical Oncology. 2022; 39: 140. https://doi.org/10.1007/s12032-022-01736-6.
- [17] Zheng X, Wang Q, Zhou Y, Zhang D, Geng Y, Hu W, et al. N-acetyltransferase 10 promotes colon cancer progression by inhibiting ferroptosis through N4-acetylation and stabilization of ferroptosis suppressor protein 1 (FSP1) mRNA. Cancer Communications. 2022; 42: 1347–1366. https://doi.org/10.1002/cac2.12363
- [18] Larrieu D, Britton S, Demir M, Rodriguez R, Jackson SP. Chemical inhibition of NAT10 corrects defects of laminopathic cells. Science. 2014; 344: 527–532. https://doi.org/10.1126/science. 1252651.
- [19] Zhang Y, Deng Z, Sun S, Xie S, Jiang M, Chen B, et al. NAT10 acetylates BCL-XL mRNA to promote the proliferation of multiple myeloma cells through PI3K-AKT pathway. Frontiers in Oncology. 2022; 12: 967811. https://doi.org/10.3389/fonc.2022.967811.
- [20] Tao W, Tian G, Xu S, Li J, Zhang Z, Li J. NAT10 as a potential prognostic biomarker and therapeutic target for HNSCC. Cancer Cell International. 2021; 21: 413. https://doi.org/10.1186/ s12935-021-02124-2.
- [21] Wu J, Zhu H, Wu J, Chen W, Guan X. Inhibition of N-acetyltransferase 10 using remodelin attenuates doxorubicin resistance by reversing the epithelial-mesenchymal transition in breast cancer. American Journal of Translational Research. 2018; 10: 256–264.
- [22] Qi P, Chen YK, Cui RL, Heng RJ, Xu S, He XY, et al. Overexpression of NAT10 induced platinum drugs resistance in breast cancer cell. Chinese Journal of Oncology. 2022; 44: 540–549. (In Chinese) https://doi.org/10.3760/cma.j.cn 112152-20211231-00986.
- [23] Kanai Y. Amino acid transporter LAT1 (SLC7A5) as a molecular target for cancer diagnosis and therapeutics. Pharmacology &



- Therapeutics. 2022; 230: 107964. https://doi.org/10.1016/j.ph armthera.2021.107964.
- [24] Hisada T, Kondo N, Wanifuchi-Endo Y, Osaga S, Fujita T, Asano T, et al. Co-expression effect of LLGL2 and SLC7A5 to predict prognosis in ERα-positive breast cancer. Scientific Reports. 2022; 12: 16515. https://doi.org/10.1038/s41598-022-20225-4.
- [25] Najumudeen AK, Ceteci F, Fey SK, Hamm G, Steven RT, Hall H, et al. The amino acid transporter SLC7A5 is required for efficient growth of KRAS-mutant colorectal cancer. Nature Genetics. 2021; 53: 16–26. https://doi.org/10.1038/ s41588-020-00753-3.
- [26] Shibasaki Y, Yokobori T, Sohda M, Shioi I, Ozawa N, Komine C, et al. Association of High LAT1 Expression with Poor Prognosis and Recurrence in Colorectal Cancer Patients Treated with Oxaliplatin-Based Adjuvant Chemotherapy. International Journal of Molecular Sciences. 2023; 24: 2604. https://doi.org/10.3390/ijms24032604.
- [27] Li C, Chen S, Jia W, Li W, Wei D, Cao S, et al. Identify metabolism-related genes IDO1, ALDH2, NCOA2, SLC7A5, SLC3A2, LDHB, and HPRT1 as potential prognostic markers and correlate with immune infiltrates in head and neck squamous cell carcinoma. Frontiers in Immunology. 2022; 13: 955614. https://doi.org/10.3389/fimmu.2022.955614.
- [28] Zhang C, Wang Y, Guo X, Wang Z, Xiao J, Liu Z. SLC7A5 correlated with malignancies and immunotherapy response in bladder cancer. Cancer Cell International. 2024; 24: 182. https://doi.org/10.1186/s12935-024-03365-7.
- [29] Li Y, Wang W, Wu X, Ling S, Ma Y, Huang P. SLC7A5 serves as a prognostic factor of breast cancer and promotes cell proliferation through activating AKT/mTORC1 signaling pathway. Annals of Translational Medicine. 2021; 9: 892. https://doi.org/10.21037/ atm-21-2247.
- [30] Huang R, Wang H, Hong J, Wu J, Huang O, He J, et al. Targeting glutamine metabolic reprogramming of SLC7A5 enhances the efficacy of anti-PD-1 in triple-negative breast cancer. Frontiers in Immunology. 2023; 14: 1251643. https://doi.org/10.3389/fi mmu.2023.1251643.
- [31] Zhang X, Chen J, Jiang S, He S, Bai Y, Zhu L, et al. N-Acetyltransferase 10 Enhances Doxorubicin Resistance in Human Hepatocellular Carcinoma Cell Lines by Promoting the Epithelial-to-Mesenchymal Transition. Oxidative Medicine and Cellular Longevity. 2019; 2019: 7561879. https://doi.org/10.1155/2019/7561879.
- [32] Balmus G, Larrieu D, Barros AC, Collins C, Abrudan M, Demir M, et al. Targeting of NAT10 enhances healthspan in a mouse model of human accelerated aging syndrome. Nature Communications. 2018; 9: 1700. https://doi.org/10.1038/ s41467-018-03770-3.
- [33] Dominissini D, Rechavi G. N⁴-acetylation of Cytidine in mRNA by NAT10 Regulates Stability and Translation. Cell. 2018; 175: 1725–1727. https://doi.org/10.1016/j.cell.2018.11.037.
- [34] Arango D, Sturgill D, Alhusaini N, Dillman AA, Sweet TJ, Hanson G, *et al.* Acetylation of Cytidine in mRNA Promotes

- Translation Efficiency. Cell. 2018; 175: 1872–1886.e24. https://doi.org/10.1016/j.cell.2018.10.030.
- [35] Dalhat MH, Mohammed MRS, Ahmad A, Khan MI, Choudhry H. Remodelin, a N-acetyltransferase 10 (NAT10) inhibitor, alters mitochondrial lipid metabolism in cancer cells. Journal of Cellular Biochemistry. 2021; 122: 1936–1945. https://doi.org/ 10.1002/jcb.30155.
- [36] Wu Y, Cao Y, Liu H, Yao M, Ma N, Zhang B. Remodelin, an inhibitor of NAT10, could suppress hypoxia-induced or constitutional expression of HIFs in cells. Molecular and Cellular Biochemistry. 2020; 472: 19–31. https://doi.org/10.1007/ s11010-020-03776-w.
- [37] Yan Q, Zhou J, Wang Z, Ding X, Ma X, Li W, et al. NAT10-dependent N⁴-acetylcytidine modification mediates PAN RNA stability, KSHV reactivation, and IFI16-related inflammasome activation. Nature Communications. 2023; 14: 6327. https://doi.org/10.1038/s41467-023-42135-3.
- [38] Zheng J, Tan Y, Liu X, Zhang C, Su K, Jiang Y, et al. NAT10 regulates mitotic cell fate by acetylating Eg5 to control bipolar spindle assembly and chromosome segregation. Cell Death and Differentiation. 2022; 29: 846–860. https://doi.org/10.1038/s41418-021-00899-5.
- [39] Chen X, Hao Y, Liu Y, Zhong S, You Y, Ao K, et al. NAT10/ac4C/FOXP1 Promotes Malignant Progression and Facilitates Immunosuppression by Reprogramming Glycolytic Metabolism in Cervical Cancer. Advanced Science. 2023; 10: e2302705. https://doi.org/10.1002/advs.202302705.
- [40] Long Y, Ren Y, Wei Q, Mobet Y, Liu Y, Zhao H, et al. NAT10-mediated RNA acetylation enhances HNRNPUL1 mRNA stability to contribute cervical cancer progression. International Journal of Medical Sciences. 2023; 20: 1079–1090. https://doi.org/10.7150/ijms.83828.
- [41] Qian BZ, Pollard JW. Macrophage diversity enhances tumor progression and metastasis. Cell. 2010; 141: 39–51. https://do i.org/10.1016/j.cell.2010.03.014.
- [42] Xia Y, Rao L, Yao H, Wang Z, Ning P, Chen X. Engineering Macrophages for Cancer Immunotherapy and Drug Delivery. Advanced Materials. 2020; 32: e2002054. https://doi.org/10.1002/adma.202002054.
- [43] Jiang S, Feng R, Tian Z, Zhou J, Zhang W. Metabolic dialogs between B cells and the tumor microenvironment: Implications for anticancer immunity. Cancer Letters. 2023; 556: 216076. https://doi.org/10.1016/j.canlet.2023.216076.
- [44] Huang W, Cao L. Targeting GABA signalling for cancer treatment. Nature Cell Biology. 2022; 24: 131–132. https://doi.org/10.1038/s41556-021-00839-y.
- [45] Németh ZH, Lutz CS, Csóka B, Deitch EA, Leibovich SJ, Gause WC, et al. Adenosine augments IL-10 production by macrophages through an A2B receptor-mediated posttranscriptional mechanism. Journal of Immunology. 2005; 175: 8260– 8270. https://doi.org/10.4049/jimmunol.175.12.8260.
- [46] Tie Y, Tang F, Wei YQ, Wei XW. Immunosuppressive cells in cancer: mechanisms and potential therapeutic targets. Journal of Hematology & Oncology. 2022; 15: 61. https://doi.org/10. 1186/s13045-022-01282-8.

